PP–PP-g-MAH–Org-MMT Nanocomposites. I. Intercalation Behavior and Microstructure

Weibing Xu,[1,3] Guodong Liang,[1] Wei Wang,[1] Shupei Tang,[1] Pingsheng He,[2] Wei-Ping Pan[3]

[1]*Department of Polymer Science and Engineering, Hefei University of Technology, Hefei, 230009 Anhui, China*
[2]*Department of Polymer Science and Engineering, University of Science and Technology of China, Hefei 230026, Anhui, China*
[3]*Material Characterization Center. Department of Chemistry, Western Kentucky University, Bowling Green, Kentucky 42101*

Received 27 February 2002; revised 29 July 2002; accepted 29 July 2002

ABSTRACT: The melt-direct intercalation method was employed to prepare poly(propylene) (PP)–maleic anhydride grafted poly(propylene) (PP-g-MAH)–organic-montmorillonite (Org-MMT) nanocomposites. X-ray diffractometry (XRD) was used to investigate the intercalation effect, crystallite size, and crystal cell parameter in these composites. Two kinds of maleated PP, with graft efficiencies of 0.6 and 0.9 wt %, and two sorts of manufacturing processes were used to prepare nanocomposites and then to investigate their effects on intercalation behavior. The results showed that the intercalation effect was enhanced by increasing the content of PP-g-MAH, using maleated PP with higher graft efficiency, and adopting the mold process. The crystallite size of nanocomposites perpendicular to the crystalline plane, such as (040), (130), (111), and (041), reached the minimum value when the content of PP-g-MAH was 20 wt %. This result indicated that the crystallite size of PP in nanocomposites decreased by proper addition of PP-g-MAH. Maximum values in tensile strength (40.2 MPa) and impact strength (24.3 J/m) were achieved when the content of PP-g-MAH was 10 and 20%, respectively. © 2003 Wiley Periodicals, Inc. J Appl Polym Sci 88: 3225–3231, 2003

Key words: poly(propylene) (PP), nanocomposites; crystal structures

INTRODUCTION

The hybrid organic–inorganic composites are promising materials because they synergistically integrate the advantages of organic polymer and inorganic material, such as, the excellent process properties that are generally considered to be characteristic of polymer, and high modulus and strength that are characteristic of inorganic material. However, the properties of the hybrid organic–inorganic composites are greatly influenced by the length scale of component phase.[1–3] Generally, the smaller are the inorganic filler particles, the more homogenously they are dispersed in polymer matrix and, to some extent, the more excellent physical and mechanical properties can be achieved. Polymer–clay nanocomposites are a class of hybrid materials composed of organic polymer matrix in which inorganic particles with nanoscale dimension are embodied.[4–7] At this scale, the inorganic fillers dramatically improve the properties of polymer even though their amount is small. These nanocomposites exhibit improved modulus, lower thermal expansion coefficient and gas permeability, higher swelling resistance, and enhanced ionic conductivity compared with the pristine polymers, presumably because of the nanoscale structure of the hybrids and the synergism between the polymer and the silicate.[8, 9] Preparing nanocomposites by intercalating layered silicates has proven to be a versatile approach to diminishing the length scale of component phase. Since a montmorillonite (one of a group of clay materials known as smectite)-reinforced nylon nanocomposite with excellent mechanic properties was developed by the Toyota group, much attention has been devoted to smectite as a reinforcement material for polymers.[10–14]

Many approaches were employed to prepare polymer–clay nanocomposites. In most cases, the preparation involves intercalation of a suitable monomer and exfoliating the layered galleries into their nanoscale elements by subsequent polymerization. However, this method requires choosing the proper monomer or certain solvent as a medium, which puts a strong restraint on the polymer used for the nanocomposites. Thus far, only some polar polymers, such as epoxide polymer,[15,16] poly(ethylene oxide) (PEO),[17] and polystyrene (PS)[18] have been used successfully. These polar polymers are successful because they can intercalate between smectite layers, from which the nanocomposite is derived. Hence, poly(propylene) (PP) with a small polarity has rarely been used successfully for nanocomposites production by this method. One

Correspondence to: W.B. Xu (xwb105105@sina.com).

Journal of Applied Polymer Science, Vol. 88, 3225–3231 (2003)

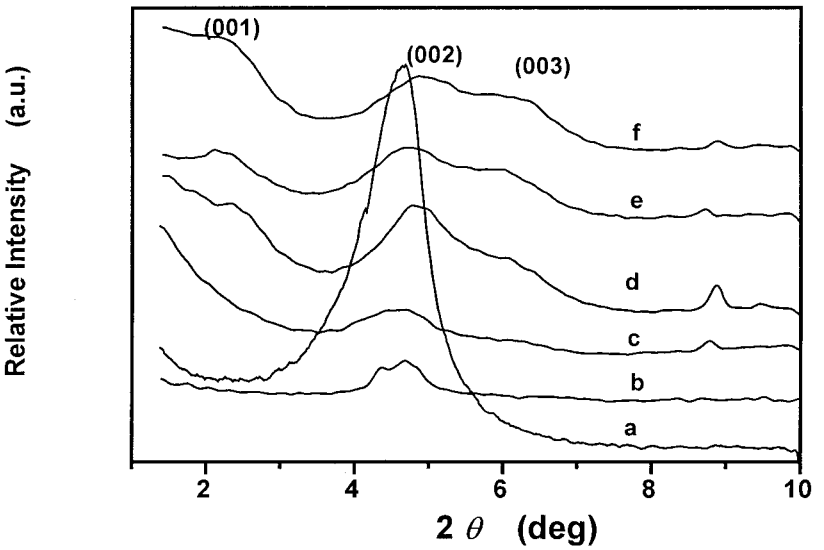

Figure 1 XRD patterns of Org-MMT (a) and PP–PP-g-MAH–Org-MMT nanocomposites with the following proportions: (b)98:0:2, (c) 92:6:2, (d) 98;10:2, (e) 78:20:2, and (f) 68:30:2 (PP-g-MAH with graft efficiency of 0.6 wt %; mold process).

promising approach to such nanocomposite production is by direct polymer melt intercalation processing, which is simple to operate and friendly to the environment. Many polymer systems (e.g., PS, polyamide, and PEO) containing silicate have been prepared in this way.

PP is one of the most widely used polyolefin polymers. However, because it does not include any polar groups in its backbone, it was not thought that homogenous dispersion of the silicate layers in PP would be realized. In general, clay is modified with alkylammonium (the alkylammonium makes the hydrophilic clay surface organophilic) to facilitate its interaction with a polymer matrix; For examples, Kato et al. prepared PP-based nanocomposites by melt blending three components [PP, PP–maleic acid (PP–MA), and modified clay] in a twin-screw extruder,[19,20] and Wolf described that swollen organomodified clay was compounded with PP in a twin-screw extruder at 250°C to yield PP–organomodified clay nanocomposites.[21] In our previous studies, PP–organic-montmorillonite (PP–Org-MMT) nanocomposites were obtained by direct melt blending of a special brand of PP and Org-MMT.[13,22]

In this study, another brand of PP was used, and PP–maleic anhydride-grafted PP–Org-MMT (PP–PP-g-MAH–Org-MMT) nanocomposites were synthesized successfully by a different direct melt intercalation process (i.e., a mold or injection process). The crystallite size and crystal cell parameters of PP–PP-g-MAH–Org-MMT nanocomposites were investigated by X-ray diffraction (XRD) analysis. In addition, the mechanical properties of the PP–PP-g-MAH–Org-MMT composites were examined.

TABLE I
2θ and *d* Values for Org-MMT and PP/PP-g-MAH (With Graft Efficiency of 0.6 wt %)/Org-MMT Nanocomposites (Mould Process)

	2θ (deg)		*d* (nm)	
PP/PP-g-MAH/org-MMT	(001)	(002)	(001)	(002)
0/0/100	4.64	—	1.90	—
98/0/2	4.60	—	1.92	—
92/6/2	4.5	—	1.96	—
88/10/2	2.46	4.84	3.59	1.82
78/20/2	2.32	4.72	3.80	1.87
68/30/2	2.30	4.90	3.84	1.80

EXPERIMENTAL

Materials

Poly(propylene) (PP; FY4012 brand) used was purchased from The Polyolefin Company, Ltd. (Singapore) and used without any treatment. Maleated poly(propylene) [i.e., maleic anhydride-grafted PP (PP-g-MAH)], with graft efficiencies of 0.6 and 0.9 wt %, were prepared by reactive extrusion in our own laboratory.[23] Na^+-Montmorillonite was available from Lin'an Chemistry Agent Factory (China), and organic-montmorillonite (Org-MMT) was synthesized in our own laboratory according to a previously published procedure.[24]

Preparation of PP–PP-g-MAH–Org-MMT

Mold process

PP-g-MAH and Org-MMT were melt mixed in roller mill at 175–180°C for 15 min under prescribed conditions to make a master batch. Then, the master batch

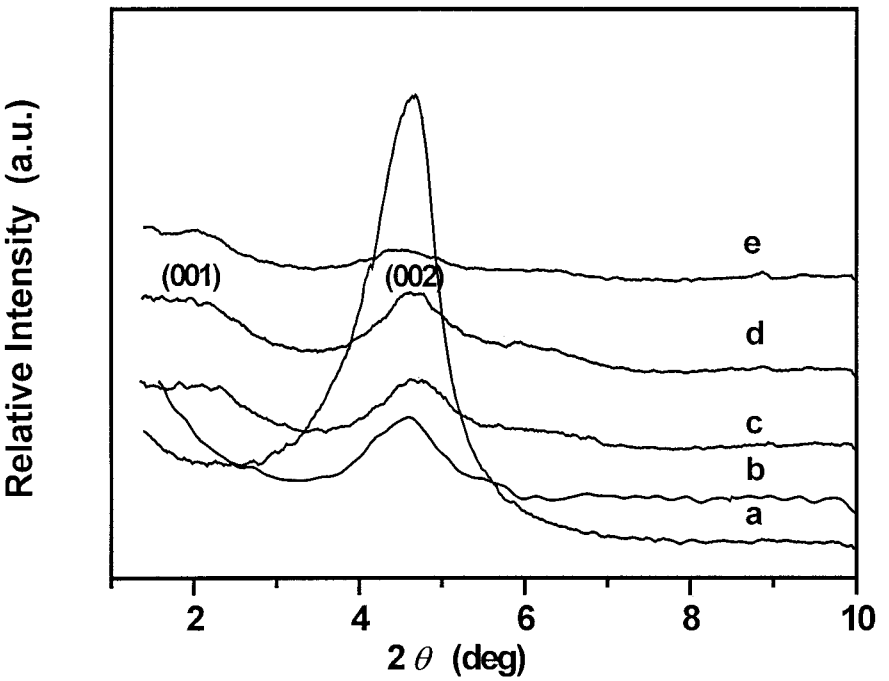

Figure 2 XRD patterns of Org-MMT(a) and PP–PP-g-MAH–Org-MMT composites with the following proportions: (b)98:0:2, (c) 92:6:2, (d) 98;10:2, (e) 78:20:2, and (f) 68:30:2 (PP-g-MAH with graft efficiency of 0.9 wt %; mold process).

and conventional PP were melt mixed under prescribed conditions in a roller mill at 175–180°C for 15 min. The resulting sheet was compression molded at 180°C for 30 min into a plate with a thickness of 4 mm.

Injection process

The master batch and conventional PP were melt mixed in a screw extruder (SJ-45B) with a rotational speed of 24 r/min. The resulting extrudate was cooled with cool water, and then was cut into pellet that was kept in oven for 4 h at 80°C. The resulting particle was injected into a measuring sample in a plastics injection machine (XS-ZY-125A).

Measurements

X-ray diffraction analysis (XRD) was carried out to confirm whether the PP–PP-g-MAH–Org-MMT nanocomposites were formed and investigate the intercalation effect of the nanocomposites. A D/max-γB diffractometer was employed, with Cu-Kα radiation and graphite filter, at room temperature. The XRD patterns were scanned in the 2θ range 1.2–10° at a rate of 1°/min. The interlayer distance of Org-MMT in composites was calculated from the (001) peak with the Bragg equation. The D/max-γB diffractometer was also employed to certify the crystal type of PP in the mentioned composites and to investigate the change of crystallite size and crystal cell parameters of PP in the composites. The diffractograms were scanned in the 2θ range 2.2–30° and at a rate of 2°/min.

The tensile test was carried out with a Model LJ-1000 testing machine at a crosshead speed of 50 mm/min at room temperature. The Izod impact test was examined with a Model IZODUJ-4 impact testing machine at room temperature according to GB1040-1996 and GB1843-1986. The specimens used were prepared with a vulcanization machine (QLB400 × 400 × 2) by compression molding.

TABLE II
2θ and *d* Values for Org-MMT and PP/PP-g-MAH (With Graft Efficiency of 0.9 wt %)/Org-MMT Nanocomposites (Mould Process)

	2θ/deg		d/nm	
PP/PP-g/MAH/Org-MMT	(001)	(002)	(001)	(002)
0/0/100	4.64	—	1.90	—
98/0/2	4.62	—	1.91	—
88/10/2	2.36	4.74	3.74	1.86
78/20/2	2.20	4.66	4.01	1.89
68/30/2	2.14	4.50	4.12	2.14

RESULTS AND DISCUSSION

Effect of the amount of PP-g-MAH on intercalation behavior

The XRD patterns of PP–PP-g-MAH–Org-MMT composites are shown in Figure 1 and the XRD parameters calculated form the (001) peaks are summarized in Table I. When the content of PP-g-MAH was >10 wt % in the PP–PP-g-MAH–Org-MMT composites, the (001)

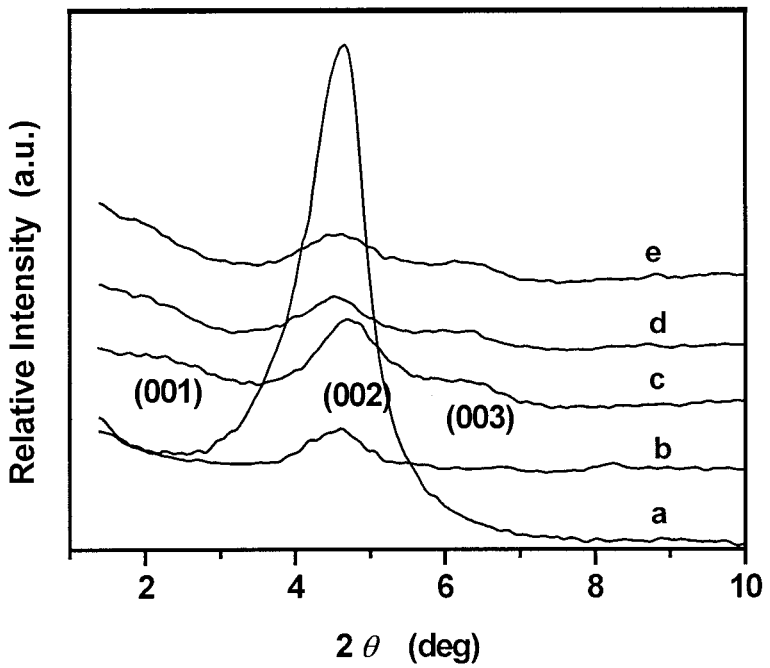

Figure 3 XRD patterns of Org-MMT(a) and PP–PP-g-MAH–Org-MMT composites with the following proportions: (b)98:0:2, (c) 92:6:2, (d) 98;10:2, (e) 78:20:2, and (f) 68:30:2 (PP-g-MAH with graft efficiency of 0.9 wt %; injection process).

plane peaks of Org-MMT at $\sim 2\theta = 4.6°$ in the XRD patterns, as expected, were shifted to lower angles of $\sim 2\theta = 2.3°$. These results mean that the interlayer distance was increased from 1.9 to 3.8 nm, which clearly indicates that macromolecule chains had intercalated into the galleries of Org-MMT. However, the result is quite different from that which occurred when the content of PP-g-MAH was <10 wt %; that is, the (001) peak of Org-MMT did not shift. This result indicates that the nonpolar macromolecule segments of PP can hardly intercalate into the interlayers of Org-MMT and that adding PP-g-MAH to the PP–Org-MMT composite is the key to preparing nanocomposites based on PP and Org-MMT. Moreover, the interlayer distance of PP–PP-g-MAH–Org-MMT increased with increasing the content of PP-g-MMT in PP–PP-g-MAH–Org-MMT, but the trend became insufficient when the content of PP-g-MAH was >20 wt %, which indicated that the intercalation effect of PP–PP-g-MAH–Org-MMT could be enhanced by increasing the content of PP-g-MAH. This enhancement of intercalation can be explained as follows: when a small amount of PP-g-MAH is included in PP–PP-g-MAH–Org-MMT, instead of intercalating into interlayers of Org-MMT, the macromolecule links of PP-g-MAH wrap around the particle of Org-MMT. Only when adequate PP-g-MAH is present in PP–PP-g-MAH–Org-MMT does Org-MMT begin to be intercalated. However, when PP-g-MAH is adequate for amply intercalating interlayers of Org-MMT, increasing the amount of PP-g-MAH will not further contribute to intercalation effect of PP–PP-g-MAH–Org-MMT.

TABLE III
2θ and d Values for Org-MMT and PP/PP-g-MAH (With Graft Efficiency of 0.9 wt %)/Org-MMT Nanocomposites (Injection Process)

	2θ/deg		d/nm	
PP/PP-g-MAH/Org/MMT	(001)	(002)	(001)	(002)
0/0/100	4.64	—	1.90	—
98/0/2	4.58	—	1.93	—
88/10/2	2.60	4.82	3.39	1.82
78/20/2	2.40	4.52	3.68	1.95
68/30/2	2.20	4.50	4.01	1.96

Effect of graft efficiency of PP-g-MAH on the intercalation behavior

Maleated PP with 0.9 wt % grafted MA was used to synthesize PP–PP-g-MAH–Org-MMT nanocomposites to compare with maleated PP with 0.6 wt % grafted MA. As seen in Figure 2 and Table II, with increasing content of PP-g-MAH, the intercalation behavior in PP–PP-g-MAH–Org-MMT (with PP-g-MAH graft efficiency of 0.9 wt %) performed according to the same rule as did PP–PP-g-MAH–Org-MMT (with PP-g-MAH graft efficiency of 0.6 wt %) shown in Figure 1 and Table I. However, under certain conditions, the (001) plane peak for PP–PP-g-MAH–Org-MMT (with PP-g-MAH graft efficiency of 0.9 wt %) occurred at smaller angle than that of PP–PP-g-MAH–Org-MMT (with PP-g-MAH graft efficiency of 0.6 wt %). This result indicated that higher MAH graft effi-

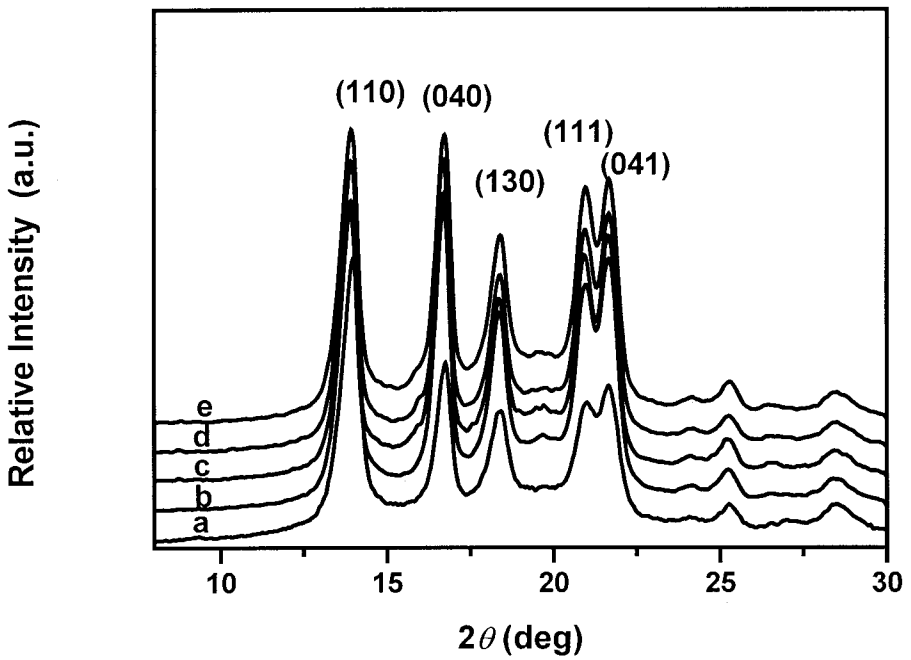

Figure 4 XRD patterns for PP(a) and PP–PP-g-MAH–Org-MMT nanocomposites with the following proportions: (b)98:0:2, (c) 92:6:2, (d) 98;10:2, (e) 78:20:2, and (f) 68:30:2 (PP-g-MAH with graft efficiency of 0.6 wt %; mold process).

ciency of PP-g-MAH will contribute to a better intercalation effect. This improved intercalation effect can be explained as follows: more polar groups, with higher graft efficiency, are included in PP-g-MAH, and these polar groups perform a very important role during the intercalation process. These results are consistent with those of a previous report.[25]

Effect of manufacturing process on intercalation behavior

PP–PP-g-MAH–Org-MMT (with PP-g-MAH graft efficiency of 0.9 wt %) nanocomposites prepared by the injection process were compared with those prepared by the mold process. As shown in Figure 3 and Table III, with increasing the content of PP-g-MAH, the intercalation behavior of PP–PP-g-MAH–Org-MMT made by the injection process is consistent with that observed in nanocomposites made by the mold process. Under certain conditions, the interlayer distance using the injection process was smaller than that in PP–PP-g-MAH–Org-MMT composites made by the mold process. This difference can be explained as follows: in the mold process, the polymer molecule remained in a high temperature for a longer time and macromolecule segments were allowed more time to disperse into interlayers of Org-MMT.

Microstructure of PP–PP-g-MAH–Org-MMT nanocomposites

To investigate the effect of Org-MMT on the crystallization of PP, diffractograms were scanned in the range 2.2–30° at a rate of 2°/min. The diffractograms, presented in Figure 4, show that the peak position of every crystal plane did not shift just because of addition of Org-MMT and PP-g-MAH. This result indicates that the crystal type of PP did not change; that is, PP remained as a monoclinic crystal type. Basing on Scherrer's equation

TABLE IV
Crystallite Size and Crystal Cell Parameters of PP and PP/PP-g-MAH (With Graft Efficiency of 0.6 wt %)/Org-MMT Nanocompostie by Mould Process

	Crystalline thickness /nm					*Crystal cell parameter*			
PP/PP-g-MAH/Org/MMT	L_{110}	L_{040}	L_{130}	L_{111}	L_{041}	a/nm	b/nm	c/nm	β/°
100/0/0	8.900	11.303	10.885	11.867	10.541	0.677	2.113	0.654	99.11
98/0/2	8.617	11.166	10.744	11.723	10.383	0.671	2.113	0.647	98.42
88/10/2	8.617	9.926	10.331	10.786	10.383	0.670	2.110	0.648	98.57
78/20/2	8.904	9.571	9.592	10.786	10.000	0.671	2.111	0.643	98.21
68/30/2	9.211	9.926	10.331	11.235	10.000	0.670	2.107	0.649	96.68

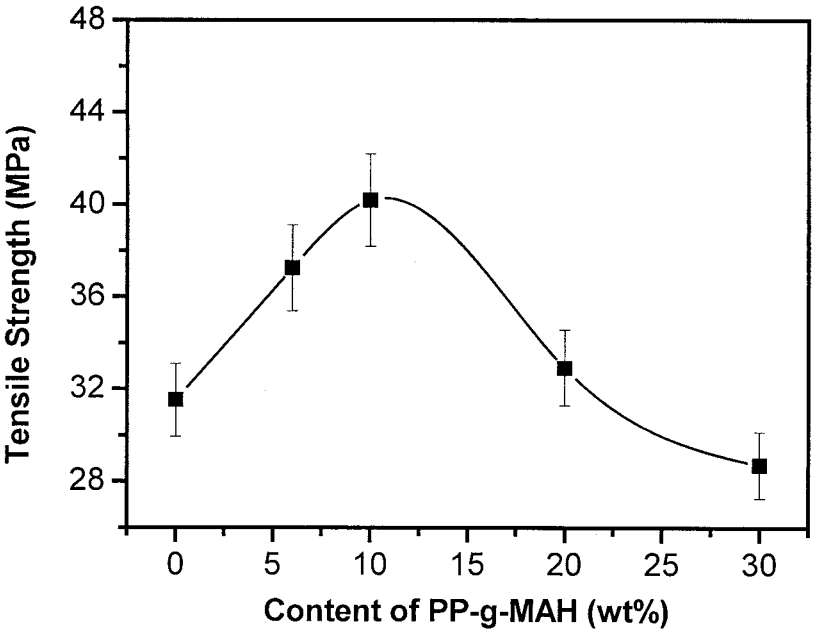

Figure 5 Plot of tensile strength versus concentration of PP-g-MAH. The mass percent of Org-MMT was 2%.

$$L_{hkl} = \frac{K\,\lambda}{\beta_0 \cos\,\theta} \quad (1)$$

where L_{hkl} is the crystallite size perpendicular to the reflection plane (hkl) (nm), θ is the Bragg angle, λ is the wavelength of X-ray used (nm), β_0 is the width of the diffraction beam used (rad), K is a shape factor of crystallite size that is related to the shape of the crystallite, and $\beta_0 = L_{hkl.}$ When β_0 is defined as the half-height width of the diffraction peaks, $K = 0.9$, then the crystallite size L_{hkl} of PP can be calculated. These results are summarized in Table IV. Employing the following equation,

$$\frac{1}{d_{hkl}^2} = \frac{1}{\sin\,\beta}\left(\frac{h^2}{a^2} + \frac{k^2 \sin^2\beta}{b^2} + \frac{l^2}{c^2} - \frac{2hl\cos\beta}{ac}\right) \quad (2)$$

the crystal cell parameters of PP and composites can be calculated. The results, shown in Table IV, indicate that the crystallite size perpendicular to the crystal plane [e.g., (040), (130), (111), and (041)] decreases first and then increases. When the content of PP-g-MAH was 20 wt %, the crystallite size reached a minimum value. This result clearly indicates that the crystallite size of the nanocomposite decreased by adding the proper amount of PP-g-MAH. This result can be explained as follows: PP-g-MAH and Org-MMT, acting as a heterogeneous nucleating agent during crystallization of PP from melt, are inclined to absorb macromolecule segments whose movement is constrained and to initiate crystallization.[13] As a result, the mechanical properties of the nanocomposites can be enhanced. In contrast, the content of PP-g-MAH had an insignificant effect on the crystal cell parameter in the nanocomposites.

Mechanical properties of PP–PP-g-MAH–Org-MMT

The effects of the amount of PP-g-MAH on tensile strength and impact strength of PP–Org-MMT are shown in Figures 5 and 6, respectively. The tensile strength and impact strength increased first and then decreased. Maximum values in tensile strength (40.2 MPa) and impact strength (24.3 J/m) were achieved when the content of PP-g-MAH was 10 and 20%, respectively. With increasing the content of PP-g-MAH, the macromolecule began to intercalate between the layers of silicate (Fig. 1 and Table I). As a result, the effective contact area between polymer and silicate increased and the tensile strength of PP–PP-g-MAH–Org-MMT composites increased. However, with further increases in the content of PP-g-MAH, the tensile strength of PP–PP-g-MAH–Org-MMT decreased. The change in impact strength was the result of the change in crystallite size due to the existence of MMT and PP-g-MAH (Table IV).

CONCLUSIONS

The following conclusions can be drawn from the results of this study. The nonpolar PP macromolecule can hardly intercalate between the interlays of Org-MMT. Adequate PP-g-MAH is necessary for preparing PP–PP-g-MAH–Org-MMT nanocomposites, and the intercalation effect of PP–PP-g-MAH–Org-MMT nanocomposites can be enhanced by increasing the

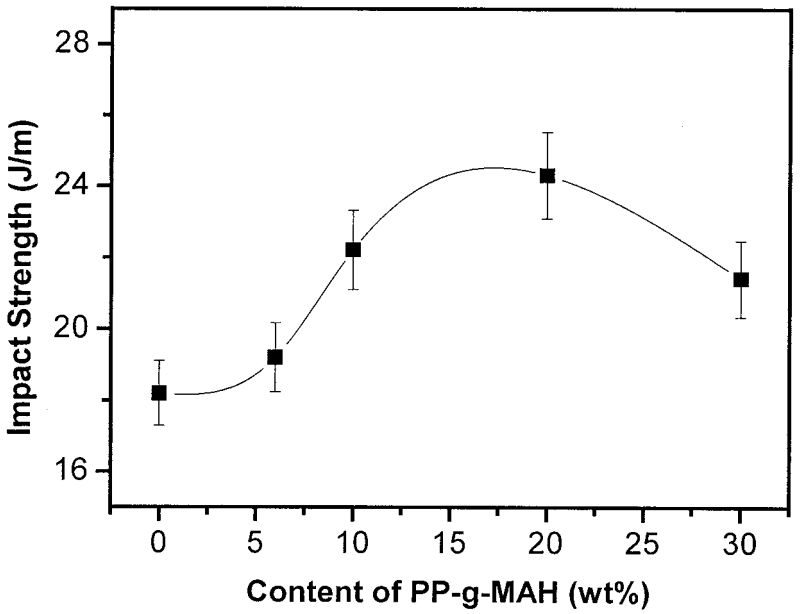

Figure 6 Plot of impact strength versus concentration of PP-g-MAH. The mass percent of Org-MMT was 2%.

content of PP-g-MAH, using maleated PP with higher MAH graft efficiency, and adopting the mold manufacturing process. The crystallite size of nanocomposites perpendicular to the crystalline plane {e.g., (040), (130), (111), and (041)] reaches the minimum value when the content of PP-g-MAH is 20 wt %. This clearly indicates that Org-MMT and PP-g-MAH have a heterogeneous nucleus effect on pure PP, which results in a decrease of crystallite size. In contrast, Org-MMT and PP-g-MAH have an insignificant effect on the crystal cell parameter of PP–PP-g-MAH–Org-MMT nanocomposites. Tensile strength and impact strength increase first and then decrease. Maximum values in tensile strength (40.2 MPa) and impact strength (24.3 J/m) are achieved when the content of PP-g-MAH is 10 and 20%, respectively. Changes in mechanical property are relative to change in interlayer distance and crystallite size in PP–PP-g-MAH–Org-MMT composites.

The authors gratefully acknowledge the financial support (Grant Number: 01402012) of the Committee of Science and Technology of Anhui Province, China.

References

1. Whiteside, G.M.; Mathias, T.P.; Seto, C.T. Science 1991, 254, 1312.
2. Gleiter, H. Adv Mater 1992, 4, 474.
3. Novak, B. Adv Mater 1993, 5, 422.
4. Messersimith, P.B.; Giannelis, E.P. J Polym Sci, Part A: Polym Chem 1995, 33, 1047.
5. Usuki, A.; Kawasumi, T.; Kojima, M.; Fukushima, Y.; Okada, A. J Mater Res 1993, 8, 1179.
6. Kojima, Y.; Usuki, A.; Kawasumi, M.; Fukushima, Y.; Okada, A.; Kurauchi, T. J Mater Res 1993, 8, 1185.
7. Yano, K.; Usuki, A.; Okada, A.; Kurauchi, T.; Kamigato, O. J Polym Sci, Part A: Polym Chem 1993, 31, 2493.
8. Giammelis, E P. Adv Mater 1996, 8, 29.
9. Wang, Z.; Piammavaia, T.J. Chem Mater 1998, 10, 3769.
10. Fukushima, Y.; Okada, A.; Kawasumi, M.; Kurauchi, T.; Kamigaito, O. Clay Miner 1988, 23, 27.
11. Kornmann, X.; Lindberg, H.; Berglund, L.A. Polymer 2001, 42, 4493.
12. Xu, W.B.; Ge, M.L.; He, P.S. J Appl Polym Sci 2001, 82, 2281.
13. Xu, W.B.; Ge, M.L.; He, P.S. China Plastics 2000, 14(11), 28 .
14. Dagani, R. Chem Eng News 1999, 77 (23), 25.
15. Wang, M.S.; Pinnavaia, T.J. Chem Mater 1994, 6, 468.
16. Messersmith, P.B.; Giannelis, E P. Chem Mater 1994, 6, 1719.
17. Vaia, R.A.; Vasudevan, S.; Krawiec, W.; Scanlon, L.G.; Giannelis, E.P. Adv Mater 1995, 7, 154.
18. Vaia, R.A.; Ishii, H.; Giannelis, E P. Chem Mater 1993, 5, 1694.
19. Kawasumi,M.; Hasegawa, N.; Kato, M.; Usuki, A.; Okada, A. Macromolecules 1997, 30, 6333.
20. Hasegawa, N.; Kawasumi, M., Kato, M.; Usuki, A.; Okada, A. J Appl Polym Sci 1998, 67, 87.
21. Wolf, D.; Fuchs, A.; Wagenknecht, U.; Kretzschmar, B.; Jehnichen, D. In Proceedings of the Eurofiller'99, Lyon-Villeurbanne, 6–9 September 1999.
22. Xu, W.B.; Ge, M.L.; He, P.S. J Polym Sci, Part B: Polym Phys 2002, 40, 408.
23 Xu, W.B.; Cai, Q.Y. J Hefei Univ Tech (Nat Sci Ed) 1992, 15(supplement), 128.
24 Xu, W.B.; Bao, S.P.; He, P.S. J Appl Polym Sci 2002, 84, 842.
25. Kato, M.; Usuki, A.; Okada, A. J Appl Polym Sci 1997, 66, 1781.